NONHSAG028908.3 sponges miR-34a-5p to promote growth of colorectal cancer via targeting ALDOA

CHUANZHUO WANG, HE XIN, GUANGXIN YAN and ZHAOYU LIU

Department of Radiology, Shengjing Hospital of China Medical University, Shenyang, Liaoning 110004, P.R. China

Received June 9, 2022; Accepted October 5, 2022

DOI: 10.3892/or.2023.8526

Abstract. Colorectal cancer (CRC) is an aggressive tumor, whose development is considered to be modulated by certain long non-coding RNAs (lncRNAs). Therefore, the aim of the present study was to investigate the regulatory mechanism of lncRNA NONHSAG028908.3 on CRC. Data from The Cancer Genome Atlas (TCGA) database revealed that NONHSAG028908.3 was increased in CRC tissues compared with normal tissues (P<0.001). The results of reverse transcription-quantitative PCR indicated that NONHSAG028908.3 was upregulated in four types of CRC cells compared with that in NCM460, a normal colorectal cell line. MTT, BrdU, and flow cytometric assays were applied to evaluate CRC cell growth. The migratory and invasive abilities of CRC cells were detected using wound healing and Transwell assays. Silencing of NONHSAG028908.3 inhibited proliferation, migration, and invasion of CRC cells. A dual-luciferase reporter assay demonstrated that NONHSAG028908.3 served as a sponge to combine with microRNA (miR)-34a-5p. MiR-34a-5p suppressed the aggressiveness of CRC cells. The effects induced by NONHSAG028908.3 knockdown were partly reversed by inhibition of miR-34a-5p. Furthermore, miR-34a-5p, a target of NONHSAG028908.3, modulated aldolase, fructose-bisphosphate A (ALDOA) expression in a negative feedback manner. Suppression of NONHSAG028908.3 notably decreased ALDOA expression, which was rescued via silencing of miR-34a-5p. Moreover, suppression of ALDOA revealed the inhibitory action on CRC cell growth and migration. In summary, the data of the present study indicate that NONHSAG028908.3 may positively regulate ALDOA via sponging miR-34a-5p, thereby promoting malignant activities in CRC.

Correspondence to: Professor Zhaoyu Liu, Department of Radiology, Shengjing Hospital of China Medical University, 36 Sanhao Street, Shenyang, Liaoning 110004, P.R. China
E-mail: liushjh@163.com

Key words: colorectal cancer, NONHSAG028908.3, microRNA-34a-5p, aldolase, fructose-bisphosphate A

Introduction

Colorectal cancer (CRC), the third most common malignant cancer, exhibits high mortality worldwide (1). It was revealed that a total of 53,200 individuals succumbed to CRC in the United States, in 2020 (2). Although the diagnosis and treatment of CRC have improved, patients particularly those with advanced CRC still have a poor prognosis (3). Therefore, it is worth clarifying the molecular mechanism of CRC for effective treatment.

Recently, long non-coding RNAs (lncRNAs) have been demonstrated as the pivotal regulators of various tumorigenic processes such as cell proliferation, migration, and apoptosis (4-6). Research has revealed that several lncRNAs, such as lncRNA GASS, ADIPOQ, FEZF1-AS1 and GLCC1, are aberrantly expressed in CRC and play vital roles in the development of CRC (7-10). Among lncRNAs, NONHSAG028908.3 also known as LINC01123, has been demonstrated to promote cell proliferation, migration and invasion in different types of cancer, including non-small cell lung cancer, osteosarcoma and hepatocellular carcinoma (11-13), however the role of NONHSAG028908.3 in CRC progression is poorly understood. Data obtained from The Cancer Genome Atlas (TCGA) (http://cancergenome.nih.gov/) database reveals that the expression of NONHSAG028908.3 is significantly upregulated in CRC tissues compared with normal tissues (P<0.001). In addition, patients with high expression of NONHSAG028908.3 may have low survival probability. Thus, it is hypothesized that NONHSAG028908.3 contributes to the progression of CRC.

In addition, lncRNAs act as a sponge to bind with microRNAs (miRNAs or miRs), mRNA or proteins to perform biological functions (14). Studies indicate that the aberrant expression of miRNAs participates in regulating tumorigenic processes in CRC (15). For instance, Huang *et al* reported that reduced expression of miR-4319 was correlated with poor prognosis in patients with CRC, and miR-4319 suppressed CRC progression by targeting ABTB1 (16). Although some studies have revealed that miR-34a-5p is usually downregulated in CRC (17-20), relevant molecular mechanisms of miR-34a-5p in CRC have not been fully elucidated. The regulatory association between NONHSAG028908.3 and miR-34a-5p in CRC remains unclear.

Aberrant metabolism, particularly abnormal activation of the glycolytic pathway, is a general feature of cancer. Cancer cells usually exhibit increased glycolysis to produce

more energy (21). Moreover, a high rate of glycolysis has been demonstrated to be associated with a poor prognosis in patients with cancer (22). As a glycolytic enzyme, aldolase, fructose-bisphosphate A (ALDOA), has been demonstrated to be upregulated in various types of cancer (23-25). Nevertheless, the role of ALDOA in CRC is controversial. Li *et al* reported that downregulation of ALDOA promoted the migration of CRC cells (SW480 and SW620) (26). By contrast, Dai *et al* revealed that ALDOA was highly expressed in CRC tissues and was associated with a poor prognosis of CRC (27). Therefore, it is necessary to reveal the function of ALDOA in CRC. Moreover, whether NONHSAG028908.3 targets miR-34a-5p/ALDOA to regulate tumorigenic processes in CRC warrants investigation.

The present study explored the function of NONHSAG028908.3 in CRC, and further clarified its regulatory effect on the miR-34a-5p/ALDOA axis.

Materials and methods

Cell culture. The normal human colon mucosal epithelial cell line (NCM460; cat. no. CP-H040) and human CRC cell lines (LoVo, cat. no. CL-0144; HCT116, cat. no. CL-0096; and Caco-2, cat. no. CL-0050) were purchased from Procell Life Science & Technology Co., Ltd. HT-29 (cat. no. ZQ0057), a CRC cell line, was obtained from Shanghai Zhong Qiao Xin Zhou Biotechnology Co., Ltd. The cell lines used have been authenticated using STR profiling. NCM460 cells were incubated in human colonic mucosal epithelial cell complete medium (cat. no. CM-H040; Procell Life Science & Technology Co., Ltd.). HT-29 and Caco-2 cells were incubated in DMEM (cat. no. SH30022; Hyclone; Cytiva) and MEM (cat. no. 41500-067; Gibco; Thermo Fisher Scientific, Inc.) medium supplemented with 10% fetal bovine serum (FBS; cat. no. 04-011-1A, Biological Industries; Sartorius AG), respectively. The LoVo cells were incubated in Ham's F-12K (cat. no. PM150910; Procell Life Science & Technology Co., Ltd.) medium which contained 10% FBS. McCoy's 5A (cat. no. PM150710; Procell Life Science & Technology Co., Ltd.) medium including 10% FBS was used to culture HCT116 cells. Penicillin (100 U/ml) and streptomycin (0.1 mg/ml) were added into all the aforementioned media. The cells were maintained in a humidified incubator at a temperature of 37˚C and a CO_2 ratio of 5%. Cells growing in the logarithmic phase, were used in the subsequent experiments.

Cell transfection. NONHSAG028908.3 siRNAs [si-NONHSAG028908.3-1 forward (F), 5'-GCUAGAUUG CUAUAGUCUATT-3' and reverse (R), 5'-UAGACUAUAGCA AUCUAGCTT-3'; and si-NONHSAG028908.3-2 F, 5'-GAG AAGUUCUGCAGAUGUATT-3' and R, 5'-UACAUCUGC AGAACUUCUCTT-3'], ALDOA siRNA (si-ALDOA F, 5'-GGAGGAGUAUGUCAAGCGAGCTT-3' and R, 5'-UCG CUUGACAUACUCCUCCUGTT-3'); negative control (si-NC F, 5'-UUCUCCGAACGUGUCACGUTT-3' and R, 5'-ACGUGACACGUUCGGAGAATT-3'); miR-34a-5p mimics (F, 5'-UGGCAGUGUCUUAGCUGGUUGU-3' and R, 5'-AACCAGCUAAGACACUGCCAUU-3'); NC mimics (F, 5'-UUCUCCGAACGUGUCACGUTT-3' and R, 5'-ACG UGACACGUUCGGAGAATT-3'); miR-34a-5p inhibitor (F, 5'-ACAACCAGCUAAGACACUGCCA-3'); and NC inhibitor (F, 5'-UUGUACUACACAAAAGUACUG-3') were obtained from JTS scientific; http://www.jtsbio.com/. The NONHSAG028908.3-overexpressing plasmid and corresponding empty vector were prepared by General Bio Co., Ltd. Lipofectamine 2000 reagent (cat. no. 11668-019; Invitrogen; Thermo Fisher Scientific, Inc.) was used for transfection following the manufacturer's protocols.

When the degree of cell confluence reached 70%, cells in 6-well plates were cultured with serum-free medium for 1 h. Subsequently, 100 μl Opti-MEM was used to dilute 8 μl Lipofectamine 2000 reagent, which was incubated at room temperature for 5 min. A total of 100 pmol of each construct was diluted with 100 μl Opti-MEM following incubation for 5 min, and then was transfected into cells. All dilutions were performed at room temperature for 10 min. Following the addition of the dilutions to the cells for 4 h, the medium was replaced with complete medium and further incubated for 48 h.

Reverse transcription-quantitative PCR (RT-qPCR). The total RNA from cultured cells was extracted via RNzol-Total RNA isolation Kit (cat. no. RP1001; BioTeke Corporation), and the concentration of RNA was detected using an ultraviolet spectrophotometer NANO 2000 (Thermo Fisher Scientific, Inc.). MiR-34a-5p was extended with a specific loop primer, 5'-GTT GGCTCTGGTGCAGGGTCCGAGGTATTCGCACCAGAG CCAACACAACC-3'. The total RNA was reverse transcribed into complementary DNA (cDNA) using Super M-MLV reverse transcriptase (cat. no. PR6502; BioTeke Corporation). Real-time PCR was performed using SYBR Green (cat. no. S9430; MilliporeSigma). The signals were measured via Exicycler™ 96 PCR instrument (Bioneer Corporation) and the thermocycling program consisted of holding at 94˚C for 5 min, followed by 40 cycles of 15 sec at 94˚C, 25 sec at 60˚C, and 30 sec at 72˚C. Gene expression was normalized to β-actin or U6. The relative mRNA expression was calculated via the $2^{-\Delta\Delta Cq}$ method (28). All primer sequences are presented in Table I.

MTT assay. The LoVo, HCT116, and NCM460 cells ($3x10^3$ cells/well) were seeded into 96-well plates. Cells were transfected with corresponding si-NC, si-NONHSAG028908.3-1, si-NONHSAG028908.3-2, vector, NONHSAG028908.3, NC inhibitor, miR-34a-5p inhibitor, NC mimics, miR-34a-5p mimics or si-ALODA after cell adherence. The MTT reagent (0.5 mg/ml; cat. no. M-2128; MilliporeSigma) was added to the plates according to the protocol at 0, 24, 48 and 72 h, respectively. After incubation at 37˚C for 4 h, the formazan crystals were dissolved using DMSO. Subsequently, the OD values were determined using a microplate reader (ELX-800; BioTek Instruments, Inc.) at 570 nm.

BrdU analysis. The LoVo and HCT116 cells were treated with 10 μM BrdU solution (cat. no. B110731; Aladdin Biochemical Technology Co., Ltd) for 1 h at post transfection. Cells were fixed using 4% paraformaldehyde for 15 min at room temperature, and then 0.1% Triton X-100 (cat. no. ST795; Beyotime Insitute of Biotechnology) was added for 30 min. Subsequently,

Table I. Primer sequences of reverse transcription-quantitative PCR.

Gene	Primers 5'-3'
NONHSAG028908.3	F: TACTTTGCCTTGCTTACACG
	R: AGGAGCCAGTTCCAGACC
miR-34a-5p	F: TGGCAGTGTCTTAGCTGGTTGT
	R: GCAGGGTCCGAGGTATTC
ALDOA	F: CCCTGACCTTCTCCTACGG
	R: GGCTCGCTTGACATACTCCT
β-actin	F: CACTGTGCCCATCTACGAGG
	R: TAATGTCACGCACGATTTCC
U6	F: GCTTCGGCAGCACATATACT
	R: GCAGGGTCCGAGGTATTC

F, forward; R, reverse; microRNA-34a-5p, miR-34a-5p; ALDOA, aldolase, fructose-bisphosphate A.

10% goat serum (cat. no. SL038; Beijing Solarbio Science & Technology Co., Ltd.) was used for blocking at room temperature for 15 min. Accordingly, the cells were then incubated at 4˚C overnight, with anti-BrdU antibody (1:200; cat. no. 66241-1; ProteinTech Group, Inc.). Following incubation with a fluorescence secondary antibody (1:200; cat. no. A0521; Beyotime Institute of Biotechnology), the cells were stained using DAPI (cat. no. C1002; Beyotime Institute of Biotechnology). The images were captured via fluorescence microscope at a magnification of x400.

Flow cytometry. Following transfection for 48 h, $2x10^4$ cells (LoVo and HCT116) were collected and washed with PBS. Pre-cooled ethanol (concentration, 70%) was used for fixing cells at 4˚C for 12 h. Following centrifugation at 1,000 x g at 4˚C for 5 min, cells were resuspended in 500 μl cell staining buffer (cat. no. C1052-1; Beyotime Institute of Biotechnology). Subsequently, the cells were stained with propidium iodide (25 μl; cat. no. C1052-2; Beyotime Institute of Biotechnology) and RNase A (10 μl; cat. no. C1052-3; Beyotime Institute of Biotechnology) at 37˚C for 30 min in the dark according to the manufacturer's instructions. The cell cycle was then assessed via flow cytometry (NovoCyte; Agilent Technologies, Inc.) using NovoExpress software (version 1.4.1; Agilent Technologies, Inc.).

Western blotting. Proteins from cells were extracted using RIPA lysis buffer with 1% PMSF (cat. nos. P0013B and ST506, respectively; Beyotime Institute of Biotechnology). A BCA kit (cat. no. P0009; Beyotime Institute of Biotechnology) was used to assess the protein concentration. Total protein (30 μg per lane) was separated using 10-12% SDS-PAGE (cat. no. P0015; Beyotime Institute of Biotechnology) and accordingly transferred to a PVDF membrane (cat. no. LC2005; Thermo Fisher Scientific, Inc.). Subsequently, the membrane was placed in Tris-buffered saline with 1.5% Tween-20 (TBST) for 5 min, and then incubated with primary antibody anti-cyclin D1 (1:1,000; cat. no. A19038; ABclonal Biotech Co., Ltd.), anti-CDK4 (1:1,000; cat. no. A0366; ABclonal Biotech Co., Ltd.), anti-mature matrix metalloproteinase (MMP)-2 (1:1,000; 10373-2-AP; ProteinTech Group, Inc.), anti-mature MMP-9 (1:500; cat. no. 10375-2-AP; Proteintech Group, Inc.) and anti-ALDOA (1:1,000; cat. no. A1142; ABclonal Biotech Co., Ltd.) overnight at 4˚C. The membrane was washed using TBST following treatment with HRP-labeled secondary antibody (1:10,000; cat. no. SA00001-2; Proteintech Group, Inc.) at 37˚C for 40 min. ECL (cat. no. E003; 7sea Technology Co., Ltd.) was then added into membranes to visualize the protein bands. The relative density was evaluated via Gel-Pro-Analyzer software (version 4.0; Beijing Liuyi Biotechnology Co., Ltd.).

Wound healing assay. When LoVo and HCT116 cells reached 100% confluency, the medium was replaced with serum-free medium including 1 μg/ml mitomycin C (cat. no. M0503; MilliporeSigma) for 1 h. A 200-μl pipette tip was used to a scratch the layer of the cells at 0 h, and the images were captured with microscope at a magnification of x100. The cells were then incubated at 37˚C for 24 h. Subsequently, the images were captured.

Transwell assay. The invasion capabilities of LoVo and HCT116 cells were determined via 24-well Transwell chamber assays (cat. no. 3422, Corning, Inc.). LoVo and HCT116 cells were collected at 48 h post transfection. A cell suspension ($2x10^4$ cells; 200 μl without FBS) was added to the upper chamber, which was precoated with 40 μl Matrigel for 2 h at 37˚C, while the lower chamber contained 30% FBS. After the cells were incubated for 24 h, they were fixed with 4% paraformaldehyde at room temperature for 15 min. Crystal violet (0.4%; cat. no. 0528; Amresco, LLC) was used to stain the cells at room temperature for 5 min, and then the number of cells passing through the Matrigel was determined. Five fields were randomly selected for cell counting, and the experiment was repeated three times.

Dual-luciferase reporter assay. The sequences of wild-type (wt) NONHSAG028908.3 (wt-NONHSAG028908.3), mutant (mut) NONHSAG028908.3 (mut-NONHSAG028908.3), wt-ALDOA or mut-ALDOA were subcloned into pmirGLO vectors (GenScript Biotechnology Co., Ltd.; https://www.genscript.com.cn/). The molecular sequences were as follows: wt-NONHSAG028908.3, 5'-CCCAUCAGCAGCCACUGCCC-3'; mut-NONHSAG028908.3, 5'-CCCAUGUCGUCCGUGACGGC-3'; wt-ALDOA, 5'-CACCCUUUCCGGCACACUGCCA-3'; mut-ALDOA, 5'-CACCCUUUCCGGCUGUGACGGA-3'. Accordingly, these reporter vectors with miR-34a-5p mimics or NC mimics were co-transfected into 293T cells (cat. no. ZQ0033; Shanghai Zhong Qiao Xin Zhou Biotechnology Co., Ltd.) using Lipofectamine 2000 (cat. no. 11668-019; Invitrogen; Thermo Fisher Scientific, Inc.). After 48 h, the transfected cells were harvested, and the luciferase activities were measured using the dual-luciferase reporter kit (cat. no. KGAF040; Nanjing KeyGen Biotech Co., Ltd.) normalized to *Renilla* luciferase activity.

Bioinformatics analysis. The expression pattern of NONHSAG028908.3 in CRC tissues and normal tissues was predicted using the online database, TCGA. The data of the correlation between NONHSAG028908.3 and miR-34a-5p and/or ALDOA expression levels in CRC cells or tissues were

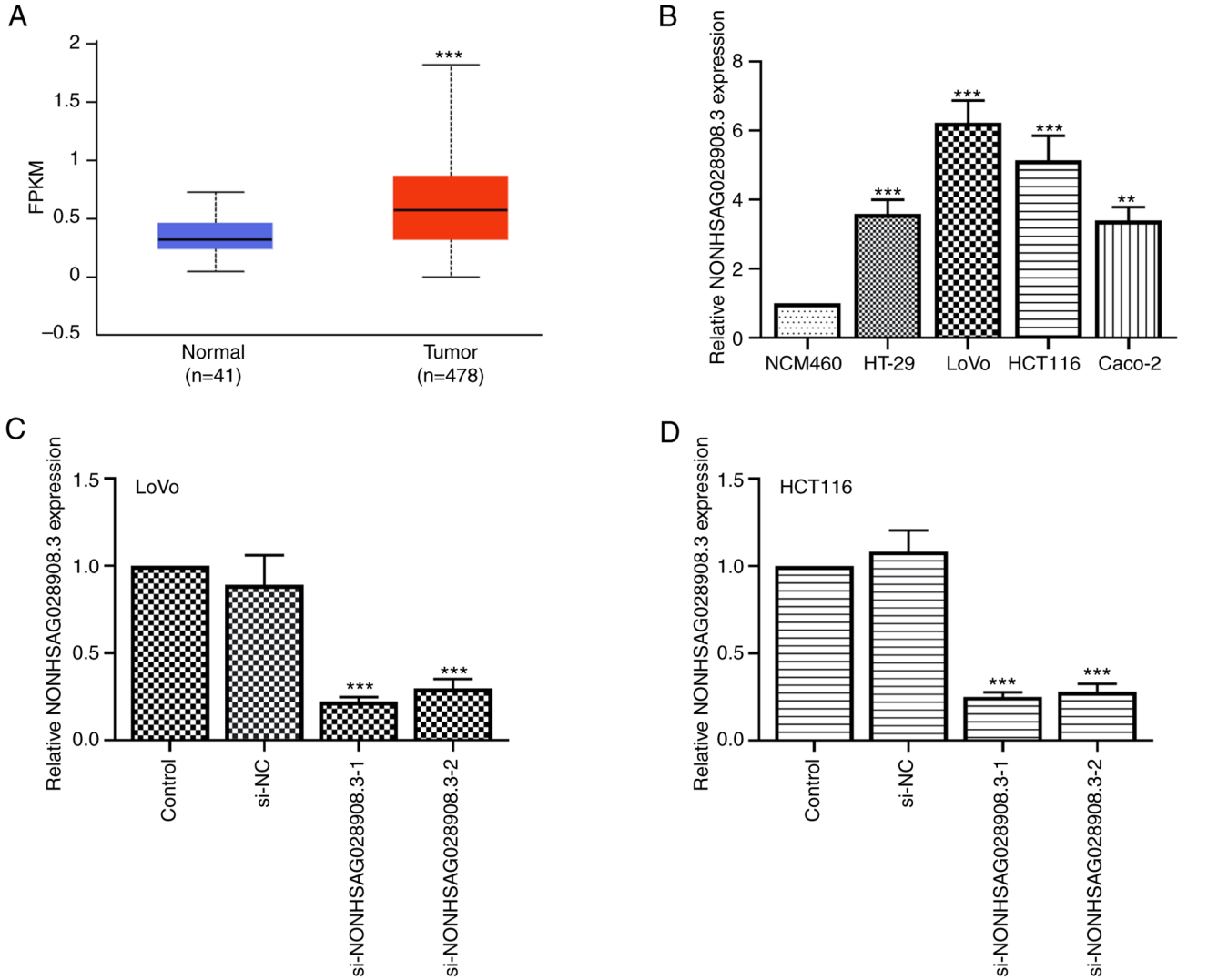

Figure 1. Expression level of NONHSAG028908.3 in CRC tissues and cells. (A) Data obtained from TCGA database revealing the expression of NONHSAG028908.3 in CRC tissues and normal tissues. (B) The relative expression levels of NONHSAG028908.3 in four CRC cell lines were detected via RT-qPCR. (C) LoVo or (D) HCT116 cells were transfected with si-NC, si-NONHSAG028908.3-1 or si-NONHSAG028908.3-2, respectively. RT-qPCR was used to evaluate the transfection efficiency. Th results are presented as the mean ± SD. **P<0.01 and ***P<0.001. CRC, colorectal cancer; TGCA, The Cancer Genome Atlas; RT-qPCR, reverse transcription-quantitative PCR; FPKM, fragments per kilobase of exon model per million mapped fragments; si-, siRNA; NC, negative control.

obtained from the Cancer Cell Line Encyclopedia (CCLE; https://sites.broadinstitute.org/ccle) and TCGA datasets.

Statistical analysis. Results were conducted using GraphPad 8.0 software (GraphPad software Inc.). The unpaired Student's t-test was performed to analyze the differences between two groups. One-way ANOVA followed by Bonferroni's post hoc test was used to analyze multiple comparisons. Pearson's correlation coefficient analysis was used to analyze correlations. Data is presented as the mean ± standard deviation (SD). P<0.05 was considered to indicate a statistically significant difference.

Results

NONHSAG028908.3 is upregulated in CRC tissues and cells. To determine the expression level of NONHSAG028908.3 (www.noncode.org) in CRC tissues and cells, TCGA database was employed and it was revealed that NONHSAG028908.3 was markedly upregulated in CRC tissues compared with that in normal tissues (Fig. 1A; P<0.001). In addition, normal colorectal cell line (NCM460) and four types of CRC cell lines were selected to determine the expression of NONHSAG028908.3 using RT-qPCR. The results revealed that the expression of NONHSAG028908.3 was also increased in HT-29, LoVo, HCT116 and Caco-2 cells compared with NCM460 cells (Fig. 1B; P<0.01). Among these cell lines, two NONHSAG028908.3 high-expressing cell lines, LoVo and HCT116, were selected to generate NONHSAG028908.3-silencing cell lines. RT-qPCR assay indicated that the expression of NONHSAG028908.3 was downregulated both in LoVo and HCT116 cells transfected with si-NONHSAG028908.3-1/2 (Fig. 1C and D; P<0.001).

Silencing of NONHSAG028908.3 suppresses the proliferation of CRC cells. To reveal the function of NONHSAG028908.3

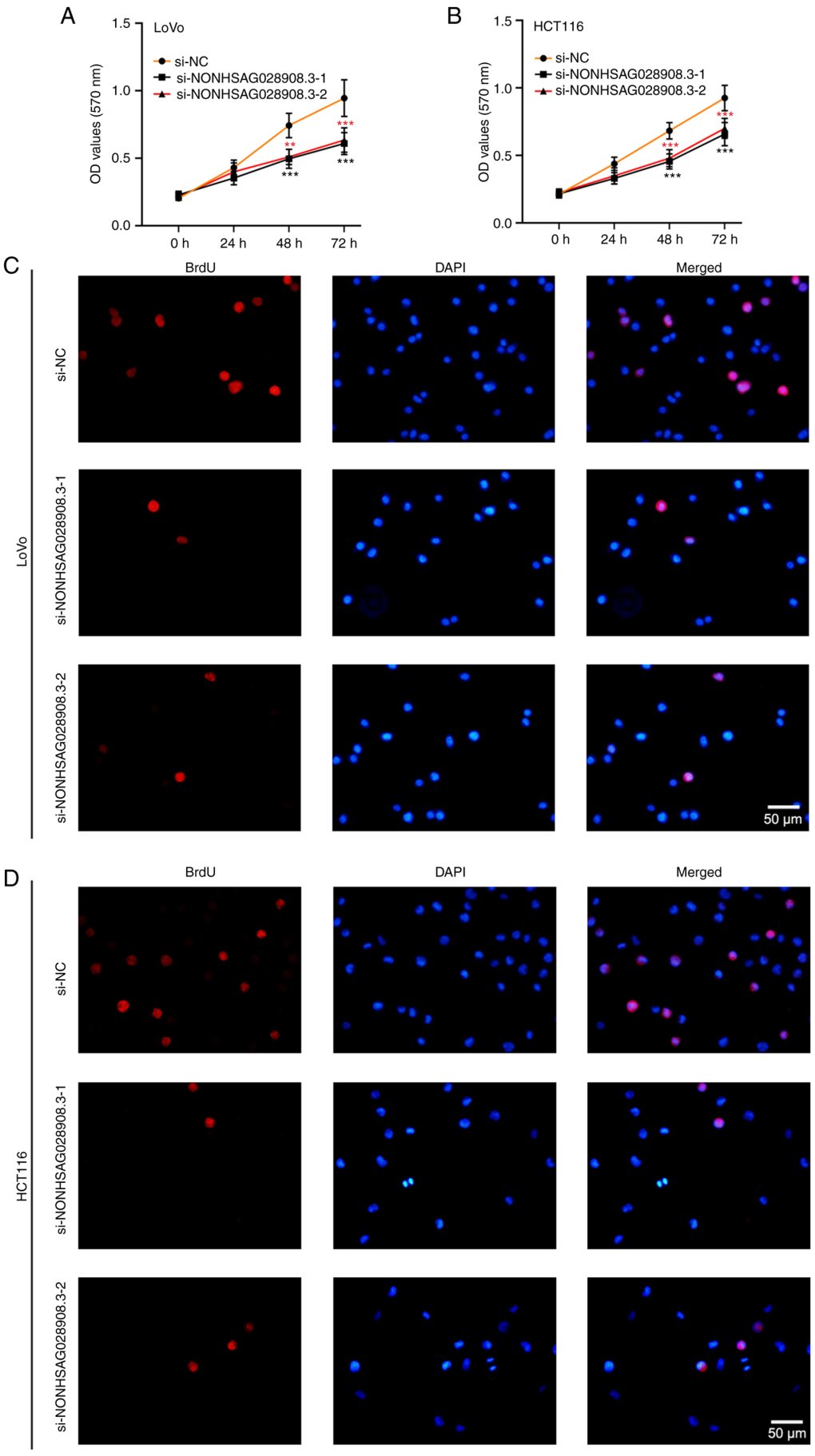

Figure 2. Silencing of NONHSAG028908.3 suppresses the cell growth of CRC cells. The cell growth of transfected LoVo and HCT116 cells was examined by (A and B) MTT assay and (C and D) BrdU staining. Scale bar, 50 μm. The results are presented as the mean ± SD. **P<0.01 and ***P<0.001. CRC, colorectal cancer; si-, siRNA; NC, negative control.

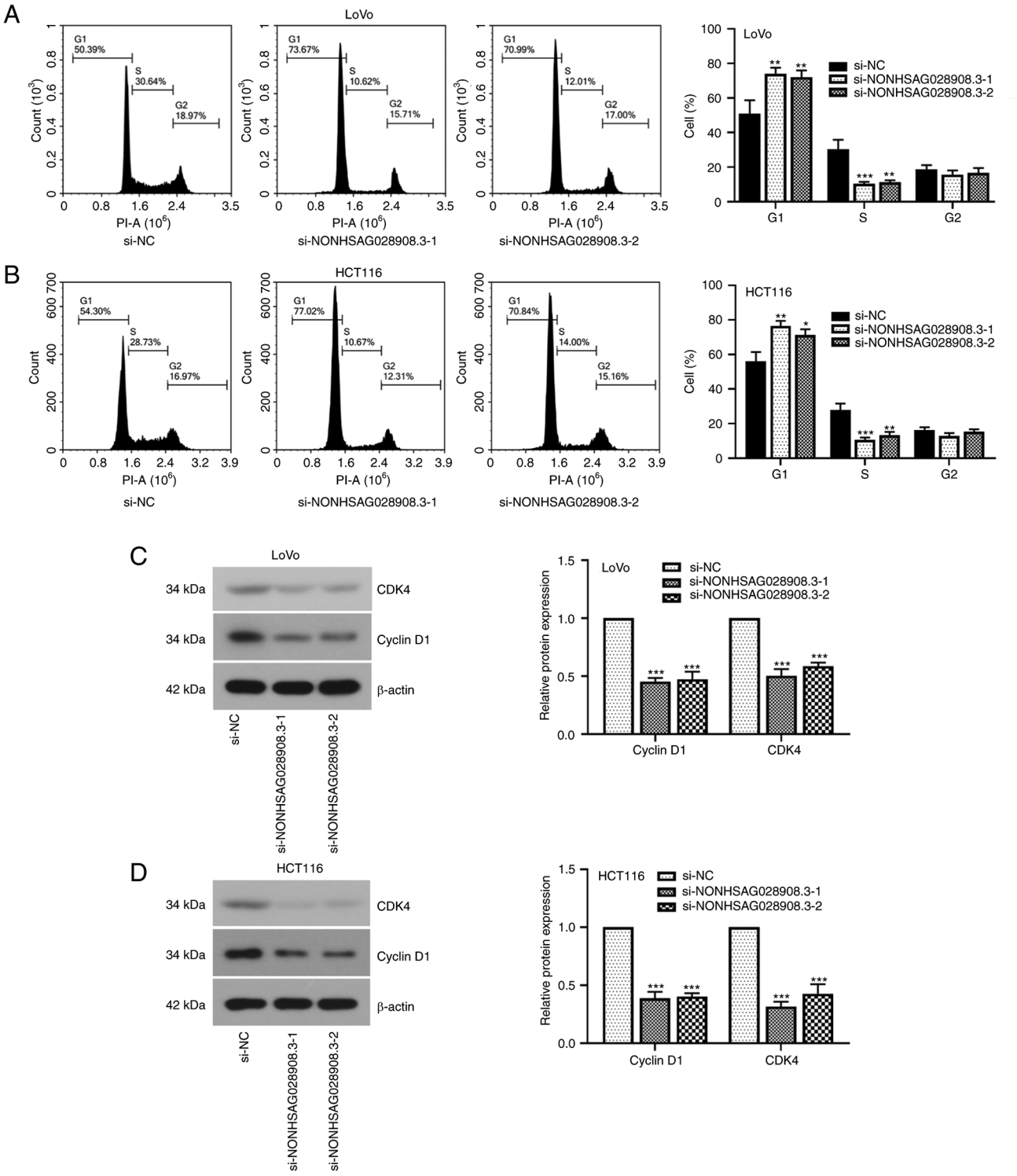

Figure 3. Silencing of NONHSAG028908.3 inhibits G1/S phase transition. Flow cytometric analysis was applied to evaluate the effect of silenced NONHSAG028908.3 on cell cycle distribution. Knockdown of NONHSAG028908.3 resulted in cell cycle arrest at the G1 phase in both (A) LoVo and (B) HCT116 cells. (C and D) Western blotting was performed to analyze the expression of CDK4 and cyclin D1. The results are presented as the mean ± SD. *P<0.05, **P<0.01 and ***P<0.001. si-, siRNA; NC, negative control.

on cell proliferation, an MTT assay was carried out on LoVo, HCT116 and NCM460 cells after transfection. The results of the MTT assay demonstrated that proliferation abilities of CRC cells (LoVo and HCT116) were decreased once transfected with the si-NONHSAG028908.3-1/2 (Fig. 2A and B; P<0.01). Overexpression of NONHSAG028908.3 promoted cell growth in NCM460 cells, a normal colorectal cell line (Fig. S1). In addition, it was found that the number of stained BrdU-positive cells was observably reduced under NONHSAG028908.3 silencing (Fig. 2C and D). In addition, the results of the flow cytometric assays demonstrated that knockdown of NONHSAG028908.3 blocked the cell cycle in the G1 phase (Fig. 3A and B; P<0.05). When the expression of NONHSAG028908.3 was inhibited, the levels

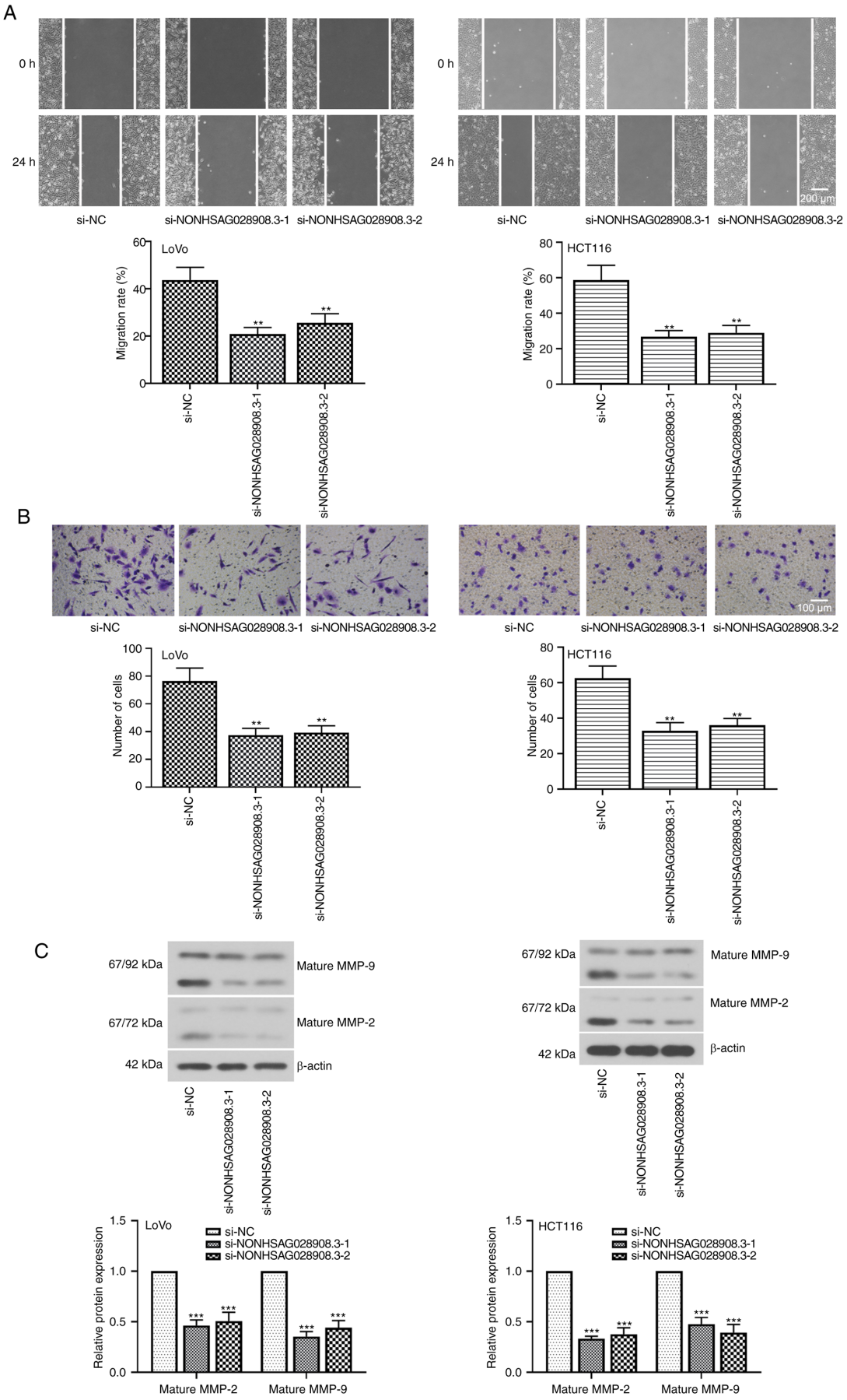

Figure 4. Knockdown of NONHSAG028908.3 restrains CRC cell migration and invasion. (A) A wound healing assay was performed to determine cell migration. Scale bar, 200 μm. (B) A Transwell assay was used to determine cell invasion. Scale bar, 100 μm. (C) The expression levels of MMP-2 and MMP-9 were assessed by western blot assay. The results are presented as the mean ± SD. **P<0.01 and ***P<0.001. CRC, colorectal cancer; MMP, matrix metalloproteinase; si-, siRNA; NC, negative control.

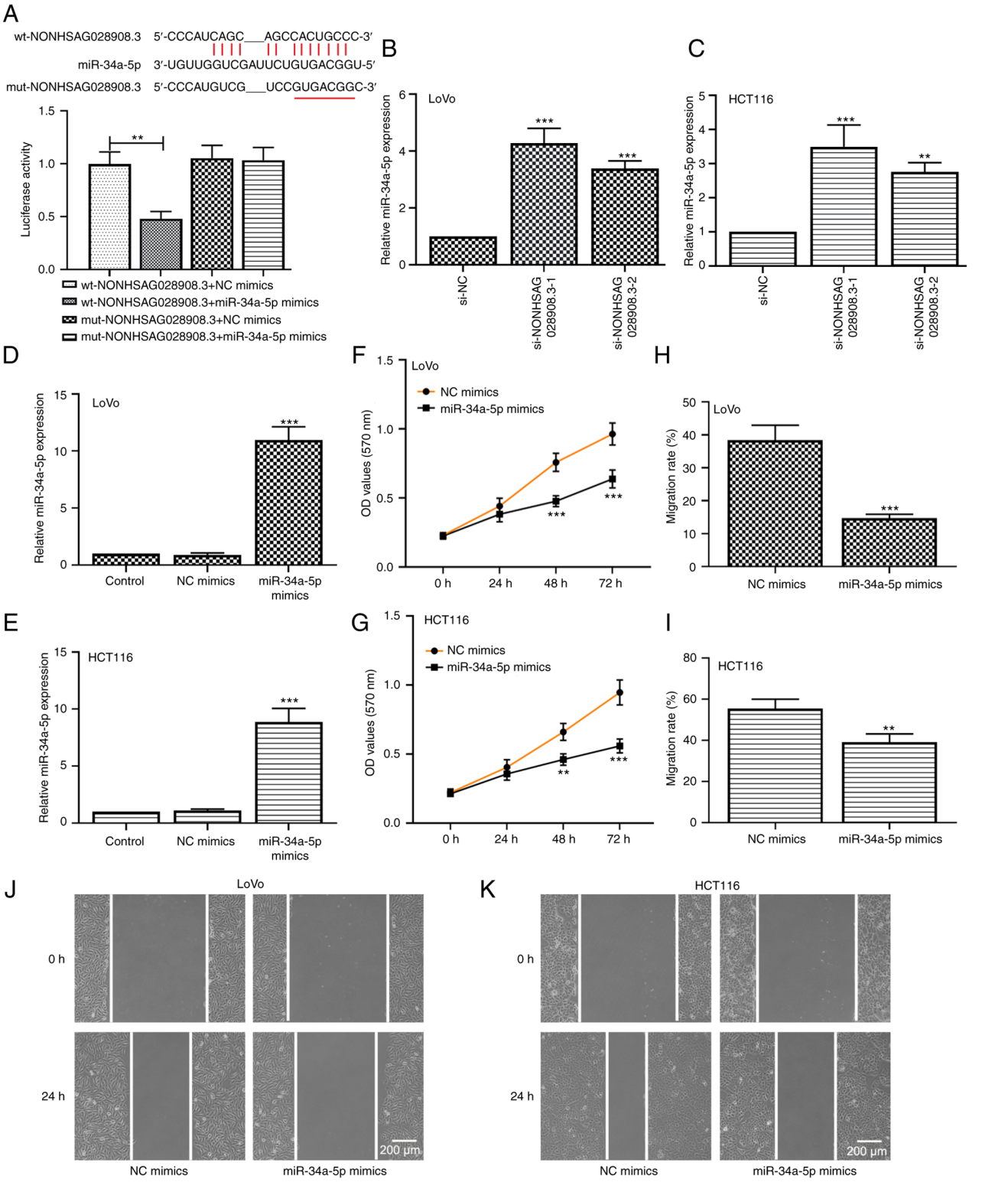

Figure 5. NONHSAG028908.3 serves as a sponge to bind to miR-34a-5p. (A) Putative binding sites between NONHSAG028908.3 and miR-34a-5p. The interaction between NONHSAG028908.3 and miR-34a-5p was confirmed by luciferase reporter assay. (B and C) RT-qPCR detected the relative expression of miR-34a-5p in LoVo and HCT116 cells transfected with si-NONHSAG028908.3. (D and E) In addition, RT-qPCR was applied to assess the expression of miR-34a-5p in LoVo and HCT116 cells transfected with miR-34a-5p mimics. (F and G) An MTT assay detected the cell growth of LoVo and HCT116 cells. (H and I) The cell migration rate of LoVo and HCT116 cells was analyzed. (J and K) The representative images of cell migration were captured. Scale bar, 200 μm. The results are presented as the mean ± SD. **P<0.01 and ***P<0.001. miR-34a-5p, microRNA-34a-5p; RT-qPCR, reverse transcription-quantitative PCR; si-, siRNA; NC, negative control.

of cell cycle-related proteins, cyclin D1 and CDK4, were downregulated in LoVo and HCT116 cells (Fig. 3C and D; P<0.001).

Knockdown of NONHSAG028908.3 restrains CRC cell migration and invasion. To further characterize the role of NONHSAG028908.3 in CRC, wound healing and Transwell

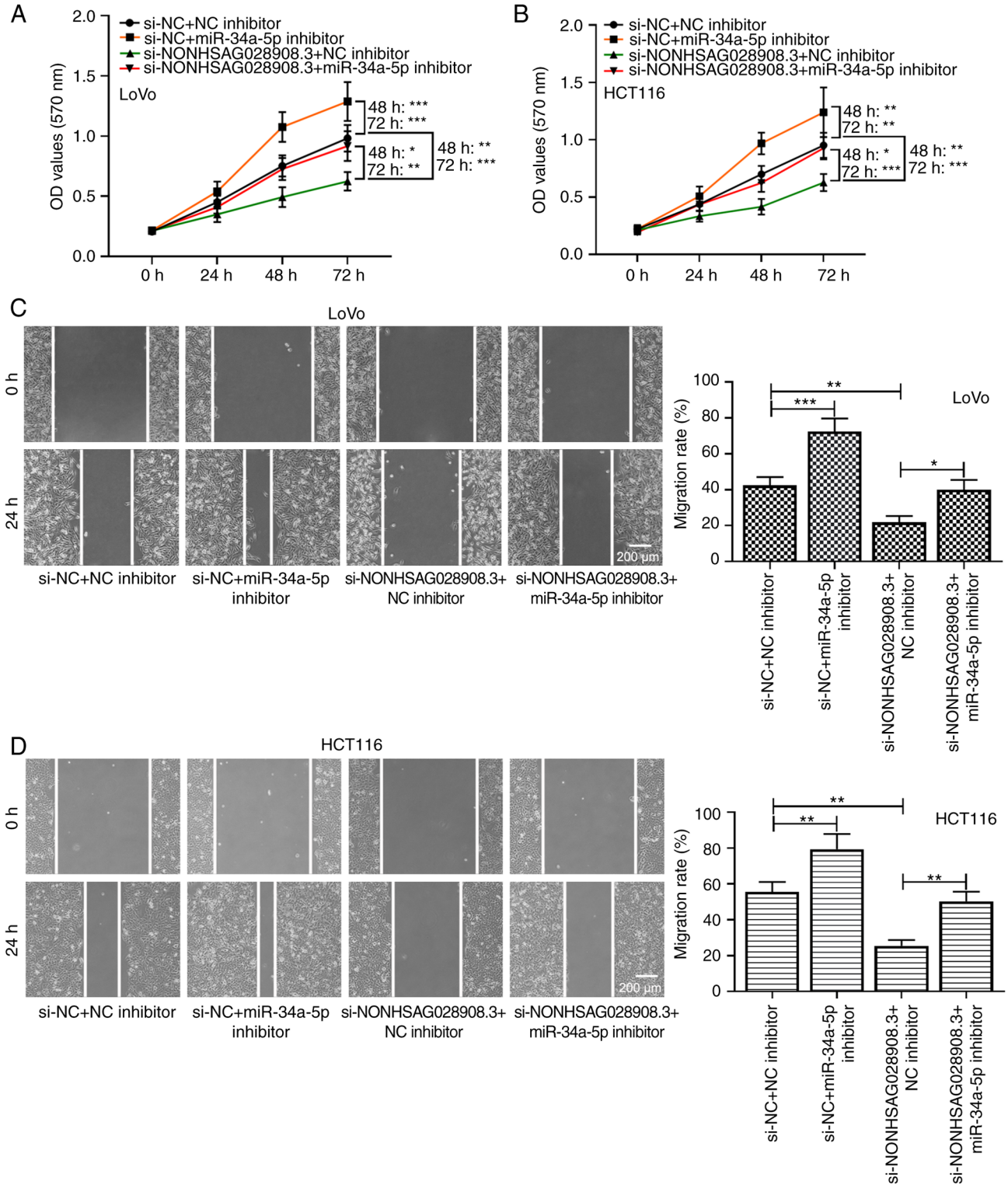

Figure 6. Suppression of miR-34a-5p abolishes the inhibitory effect of NONHSAG028908.3 knockdown on cell proliferation and migration. (A and B) LoVo and HCT116 cells were co-transfected with si-NONHSAG028908.3 and miR-34a-5p inhibitor. The OD values were examined using MTT assays at 0, 24, 48 and 72 h, respectively. (C and D) A wound healing assay was performed to assess the migration rate. Scale bar, 200 μm. The results are presented as the mean ± SD. *P<0.05, **P<0.01 and ***P<0.001. miR-34a-5p, microRNA-34a-5p; si-, siRNA; OD, optical density; NC, negative control.

assays were performed for monitoring cell migration and cell invasion, respectively. The findings of the wound healing assays revealed that the migration rate of CRC cells was significantly suppressed after inhibition of NONHSAG028908.3 (Fig. 4A; P<0.01). Similarly, the results of the Transwell invasion assays revealed that the number of cells passing through the membranes was markedly diminished when CRC cells were transfected with si-NONHSAG028908.3 (Fig. 4B; P<0.01). Furthermore, the results of the western blot assays indicated that knockdown of NONHSAG028908.3 downregulated the levels of mature MMP-2 and mature MMP-9 (Fig. 4C; P<0.001).

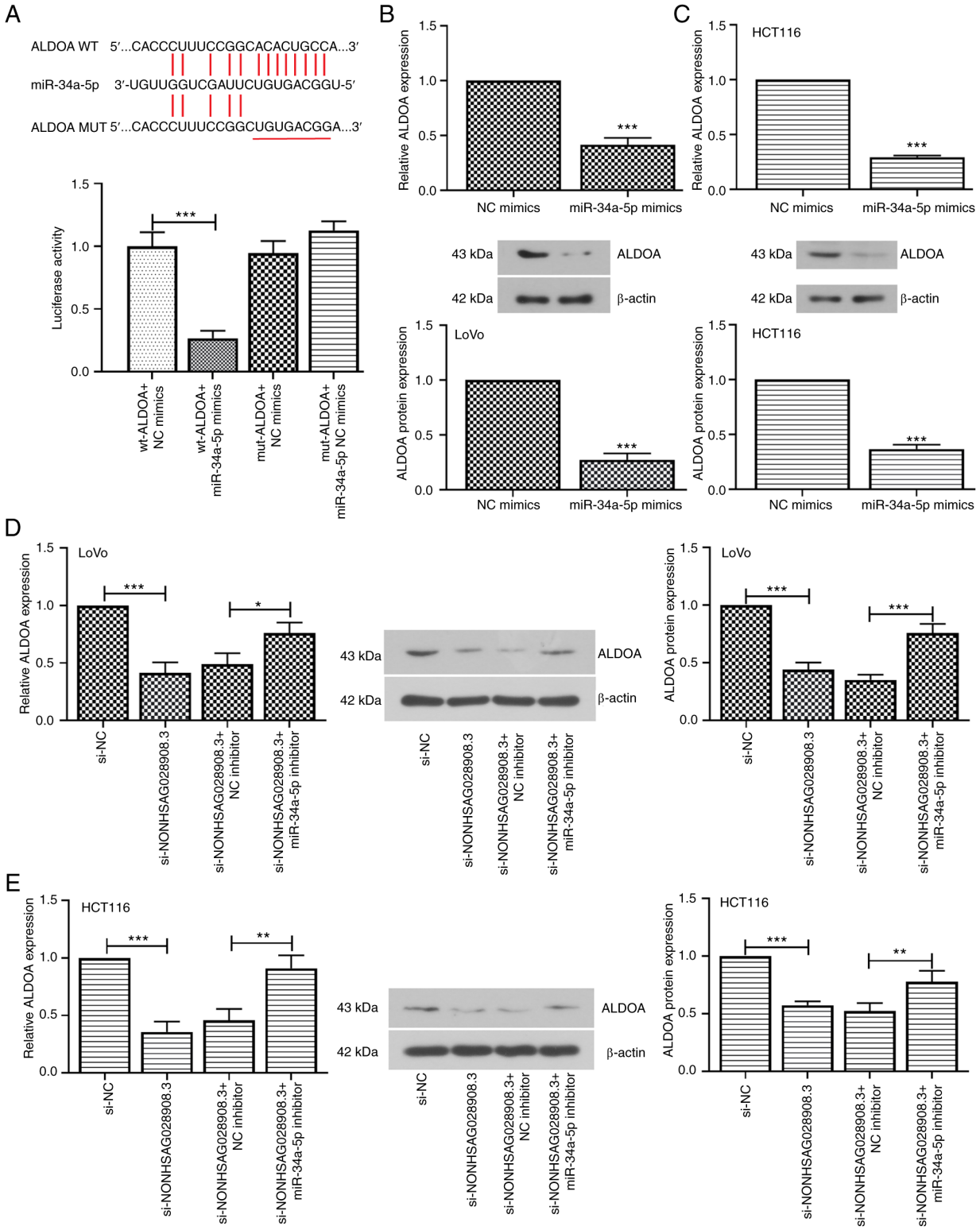

Figure 7. ALDOA is a direct target of miR-34a-5p. (A) The binding sites of miR-34a-5p to ALDOA were predicted. A luciferase assay confirmed that miR-34a-5p mimics decreased the luciferase activity of wt-ALDOA, whereas the luciferase activity of mut-ALDOA underwent no obvious change. (B and C) The LoVo and HCT116 cells were transfected with NC mimics or miR-34a-5p mimics. RT-qPCR and western blotting were used to determine the mRNA and protein expression of ALDOA, respectively. (D and E) The expression of ALDOA was detected in LoVo and HCT116 cells transfected with si-NC or si-NONHSAG028908.3 and NC inhibitor or miR-34a-5p inhibitor. The results are presented as the mean ± SD. *P<0.05, **P<0.01 and ***P<0.001. ALDOA, aldolase, fructose-bisphosphate A; miR-34a-5p, microRNA-34a-5p; wt, wild-type; mut, mutant; NC, negative control; RT-qPCR, reverse transcription-quantitative PCR; si-, siRNA.

NONHSAG028908.3 serves as a sponge to bind with miR-34a-5p. Previous research has revealed that lncRNAs can sponge miRNAs to regulate metastasis (29). In the present study, it was hypothesized that NONHSAG028908.3 served as a sponge to combine with miR-34a-5p, and their binding sites are presented in Fig. 5A. Accordingly,

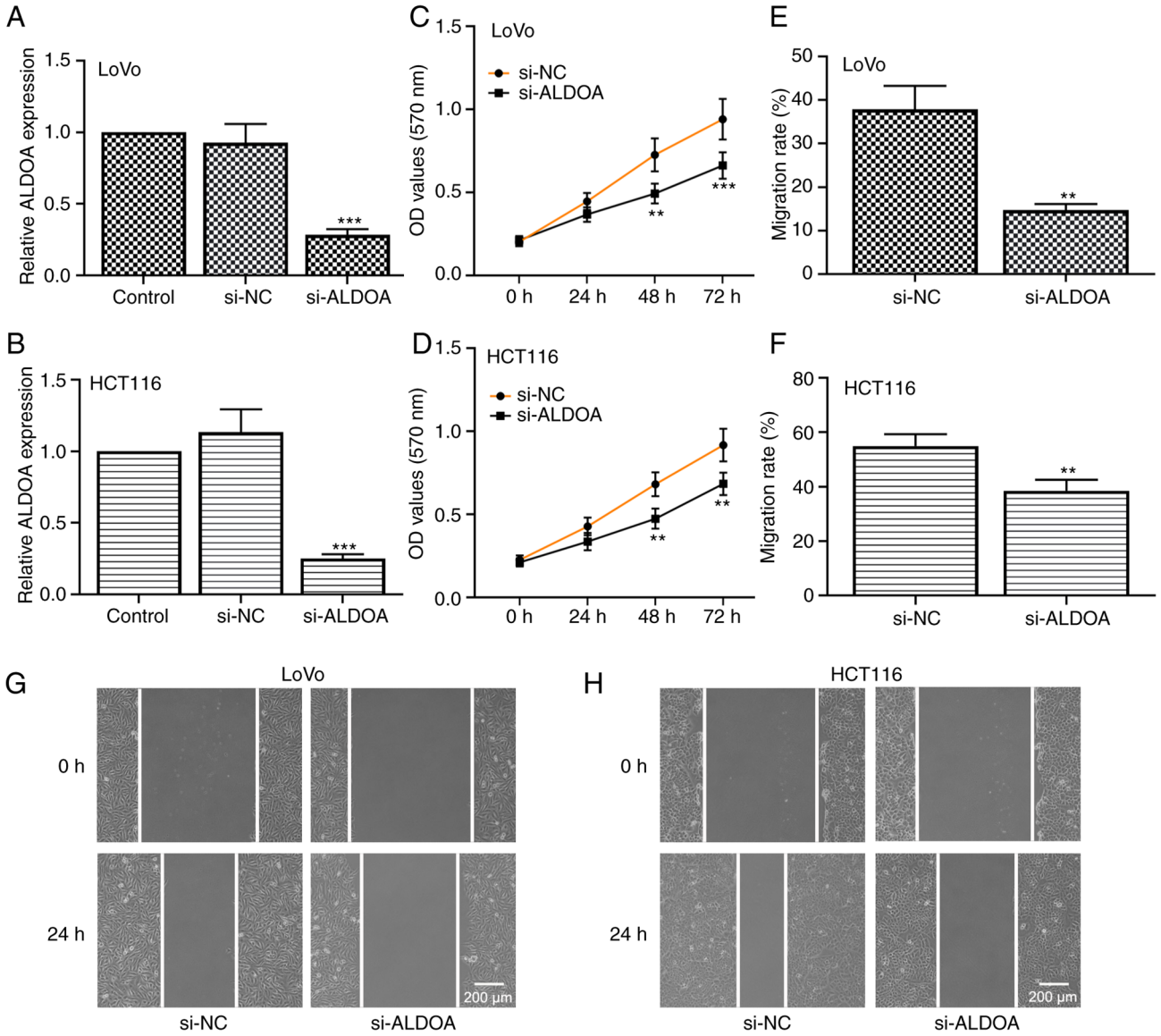

Figure 8. Knockdown of ALDOA inhibits CRC cell proliferation and migration. (A and B) Both LoVo and HCT116 cells were transfected with si-ALDOA, and the expression efficiency of ALDOA was assessed via RT-qPCR. (C and D) Cell proliferation was evaluated using MTT assay. (E and F) The cell migration rate of LoVo and HCT116 cells was analyzed. (G and H) The representative images of cell migration were captured. Scale bar, 200 μm. The results are presented as the mean ± SD. **P<0.01 and ***P<0.001. ALDOA, aldolase, fructose-bisphosphate A; CRC, colorectal cancer; si-, siRNA; RT-qPCR, reverse transcription-quantitative PCR; NC, negative control.

a luciferase reporter assay was carried out to verify the aforementioned hypothesis. The data demonstrated that miR-34a-5p mimics significantly diminished the luciferase activity of the wt-NONHSAG028908.3 reporter but did not suppress that of the mut-NONHSAG028908.3 reporter (Fig. 5A; P<0.01). Moreover, it was found that the knockdown of NONHSAG028908.3 significantly enhanced miR-34a-5p expression (Fig. 5B and C; P<0.01). These data indicated that NONHSAG028908.3 functioned as a sponge for miR-34a-5p. Additionally, the results of RT-qPCR confirmed the transfection efficiency of miR-34a-5p mimics both in LoVo and HCT116 cells (Fig. 5D and E; P<0.001). Overexpression of miR-34a-5p inhibited the CRC cell growth of LoVo and HCT116 cells according to the data of the MTT assays (Fig. 5F and G). The results of the wound healing assays demonstrated that the ability of cell migration was decreased in miR-34a-5p-overexpressing CRC cells compared with that in cells transfected with NC mimics (Fig. 5H-K).

MiR-34a-5p silencing abolishes the inhibitory effect of NONHSAG028908.3 knockdown on the malignant behavior of cells. To further explore the association between NONHSAG028908.3 and miR-34a-5p in CRC cells, rescue experiments were performed. Data from MTT assays demonstrated that the inhibitory effect of si-NONHSAG028908.3 on cell proliferation was reversed by silencing of miR-34a-5p in LoVo and HCT116 cells (Fig. 6A and B; P<0.05). Wound healing assay also confirmed this finding. In brief, NONHSAG028908.3 knockdown significantly suppressed cell proliferation and migration, whereas silencing of miR-34a-5p abolished the suppressive effect of NONHSAG028908.3 knockdown (Fig. 6C and D; P<0.05).

ALDOA directly targets miR-34a-5p and is positively correlated with NONHSAG028908.3. For the next experiment, pmirGLO luciferase reporter vectors including wt-ALDOA and mut-ALDOA were constructed. When the 293T cells were co-transfected with wt-ALDOA and miR-34a-5p mimics, the luciferase activity was significantly decreased (Fig. 7A; P<0.001). However, the luciferase activity of mut-ALDOA underwent no obvious change. Furthermore, the expression of ALDOA was assessed in miR-34a-5p-overexpressing cells. The results of RT-qPCR and western blot assays demonstrated that overexpression of miR-34a-5p negatively regulated the expression level of ALDOA in LoVo and HCT116 cells (Fig. 7B and C; P<0.001). Furthermore, knockdown of NONHSAG028908.3 significantly decreased the mRNA and protein levels of ALDOA, which were rescued via silencing of miR-34a-5p (Fig. 7D and E; P<0.05). The results obtained from TCGA and CCLE datasets revealed that the expression level of NONHSAG028908.3 was positively correlated with the expression level of ALDOA in CRC (Fig. S2; P=0.001). Collectively, these findings indicated that NONHSAG028908.3 may positively regulate ALDOA expression through sponging miR-34a-5p.

ALDOA silencing suppresses CRC cell growth and migration. Furthermore, ALDOA was successfully knocked down in LoVo and HCT116 CRC cells (Fig. 8A and B; P<0.001). The results of MTT assays demonstrated that silencing of ALDOA inhibited CRC cell proliferation (Fig. 8C and D). In addition, the migration rate of CRC cells transfected with si-ALDOA was markedly reduced compared with that in cells transfected with si-NC (Fig. 8E and H; P<0.01). Thus, the data indicated that knockdown of ALDOA suppressed CRC cell proliferation and migration.

Discussion

Although treatment of CRC has greatly improved, CRC often results in an unfavorable outcome due to the malignant metastasis of CRC cells. In consequence, researchers are urgently seeking new biomarkers for the diagnosis and prognosis of CRC. Numerous studies have demonstrated that tumor-associated genes are frequently aberrantly expressed. A number of genomes are transcribed as noncoding RNAs, of which lncRNAs and miRNAs make up the majority of noncoding RNAs (30,31). Research has revealed that lncRNAs participate in a metastatic cascade and a high abundance of cancer-related lncRNAs regulate CRC pathogenesis (32,33).

To the best of our knowledge, the function of NONHSAG028908.3 has not been fully clarified in human types of cancer. In the present study, data from TCGA database was retrieved, and the results revealed that NONHSAG028908.3 was upregulated in CRC tissues. In addition, a high level of NONHSAG028908.3 was also detected in CRC cells. Furthermore, the promoting effect of NONHSAG028908.3 on cell proliferation and migration was revealed. The aggregation of cyclin D1 and CDK4 has also been demonstrated to be of great importance in the cell cycle (34). Upregulation of cyclin D1 has been revealed to cause dysregulated CDK activity, rapid cell growth under conditions of restricted mitogenic signaling, and finally, neoplastic growth (34). In the present study it was revealed that NONHSAG028908.3 silencing led to G1 cell cycle arrest involving the alleviation of cyclin D1 and CDK4. Moreover, previous studies indicated that MMP-2 and MMP-9 accelerated cell invasion via participating in extracellular matrix degradation (35). Similarly, the data of the present revealed that inhibition of NONHSAG028908.3 suppressed cell invasion, partly by a mechanism associated to the decrease of mature MMP-2 and MMP-9. All aforementioned findings demonstrated the oncogenic property of NONHSAG028908.3 in CRC cell growth.

Mechanistic insights using a luciferase reporter assay confirmed that NONHSAG028908.3 exhibited a high affinity to interact with miR-34a-5p. It has been established that miR-34a-5p is often downregulated and plays a tumor suppressive role in multiple cancers, including CRC. Moreover, a previous study demonstrated that miR-34a-5p was downregulated in CRC tissues, and miR-34a-5p expression was positively related with disease-free survival (17). The data of the present study also confirmed that overexpression of miR-34a-5p suppressed CRC cell proliferation and migration. In addition, the findings of other studies are consistent with the findings of the present study. For instance, Li *et al* demonstrated that miR-34a-5p was negatively associated with lncARSR expression, and inhibited CRC cell invasion and metastasis (18). Gao *et al* revealed that miR-34a-5p restrained recurrence of CRC by facilitating cell apoptosis in a p53-dependent manner (17). Bao *et al* reported that inhibiting miR-34a expression aggravated CRC cell invasion via promoting epithelial-mesenchymal transition (36). Additionally, the results of the present study also revealed that depletion of NONHSAG028908.3 restrained cell proliferation and migration, which was abrogated via miR-34a-5p inhibition. This indicated that NONHSAG028908.3 served as a sponge to bind to miR-34a-5p, thus facilitating cell proliferation and migration.

Previous research demonstrated that increased glycolysis promotes cancer cell growth and survival (37). Thus, targeting glycolysis to inhibit cancer appears to be an effective method. In the present study, it was demonstrated that miR-34a-5p directly targeted ALDOA, which was regulated by NONHSAG028908.3. ALDOA, a pivotal glycolytic enzyme, acts as a catalyst in a conversion reaction of fructose-1, 6-bisphosphate (38). As aforementioned, the function of ALDOA in CRC has not been fully elucidated. Dai *et al* revealed that the expression of ALDOA was increased in CRC tissues and liver metastatic CRC tissues, and high expression of ALDOA was correlated with poor prognosis of CRC (27). Kawai *et al* demonstrated that ALDOA was positively associated with CRC cell proliferation and invasion (39). Similar to these previous studies, it was observed in the present study that ALDOA was upregulated in CRC cells (LoVo and HCT116). Knockdown of ALDOA inhibited CRC cell growth and migration. In addition, silencing of NONHSAG028908.3 attenuated the expression level of ALDOA, which was reversed by suppressing miR-34a-5p. However, Li *et al* reported that downregulation of ALDOA promoted the migration of CRC cells, SW480 and SW620 (26). Since the aforementioned study used different cells from the ones used in the present study, it is hypothesized that the different results may be caused by cell differences. In addition to ALDOA, other targets of miR-34a-5p, including TNFAIP8, flotillin-2, and hexokinase-1 have been revealed (18,40,41). Among them,

Li *et al* reported that hexokinase-1 is also the key enzyme of glycolysis and participates in CRC progression (18). However, it is not yet clear whether increased ALDOA expression is related to changes in other miR-34a-5p targets. Therefore, in future experiments, this will be investigated. In addition, lack of an animal study is a limitation of the present study. In a future study, an animal model will be established to completely confirm the function of NONHSAG028908.3 on tumor growth and metastasis *in vivo*. In addition, a sufficient number of clinical samples will be collected to further detect the expression levels of NONHSAG028908.3, miR-34a-5p, and ALDOA in CRC tissues and adjacent normal tissues, and analyze their correlation.

Collectively, the data of the present study revealed the importance of the NONHSAG028908.3/miR-34a-5p/ALDOA axis in modulating CRC progression. Upregulation of NONHSAG028908.3 was associated with the aggressive phenotypes of CRC. NONHSAG028908.3 served as a sponge to combine with miR-34a-5p and formed a positive feedback loop to regulate ALDOA. The present study provides insights into and a new mechanism for CRC treatment.

Acknowledgements

Not applicable.

Funding

The present study was supported by the National Natural Science Foundation of China (grant nos. 81470086 and 81871465).

Availability of data and materials

The datasets generated during and/or analyzed during the current study are available from the corresponding author on reasonable request.

Authors' contributions

CW performed experiments, analyzed the data and wrote the manuscript. HX and GY performed experiments and analyzed the data. ZL designed the experiments and revised the manuscript. CW and ZL confirm the authenticity of all the raw data. All authors read and approved the final manuscript and agree to be accountable for all aspects of the research in ensuring that the accuracy or integrity of any part of the work are appropriately investigated and resolved.

Ethics approval and consent to participate

Not applicable.

Patient consent for publication

Not applicable.

Competing interests

The authors declare that they have no competing interests.

References

1. Torre LA, Bray F, Siegel RL, Ferlay J, Lortet-Tieulent J and Jemal A: Global cancer statistics, 2012. CA Cancer J Clin 65: 87-108, 2015.
2. Siegel RL, Miller KD and Jemal A: Cancer statistics, 2020. CA Cancer J Clin 70: 7-30, 2020.
3. Kim C, Kim WR, Kim KY, Chon HJ, Beom SH, Kim H, Jung M, Shin SJ, Kim NK and Ahn JB: Predictive nomogram for recurrence of stage I colorectal cancer after curative resection. Clin Colorectal Cancer 17: e513-e518, 2018.
4. Bhan A, Soleimani M and Mandal SS: Long noncoding RNA and cancer: A new paradigm. Cancer Res 77: 3965-3981, 2017.
5. Forrest ME and Khalil AM: Review: Regulation of the cancer epigenome by long non-coding RNAs. Cancer Lett 407: 106-112, 2017.
6. Peng WX, Koirala P and Mo YY: LncRNA-mediated regulation of cell signaling in cancer. Oncogene 36: 5661-5667, 2017.
7. Ni W, Yao S, Zhou Y, Liu Y, Huang P, Zhou A, Liu J, Che L and Li J: Long noncoding RNA GAS5 inhibits progression of colorectal cancer by interacting with and triggering YAP phosphorylation and degradation and is negatively regulated by the m^6A reader YTHDF3. Mol Cancer 18: 143, 2019.
8. Tang HQ, Meng YL, Lu QL, Dou YY, Liang LL and Luo Y: Decreased long noncoding RNA ADIPOQ promoted cell proliferation and metastasis via miR-219c-3p/TP53 pathway in colorectal carcinoma. Eur Rev Med Pharmacol Sci 24: 7645-7654, 2020.
9. Bian Z, Zhang J, Li M, Feng Y, Wang X, Zhang J, Yao S, Jin G, Du J, Han W, *et al*: LncRNA-FEZF1-AS1 promotes tumor proliferation and metastasis in colorectal cancer by regulating PKM2 signaling. Clin Cancer Res 24: 4808-4819, 2018.
10. Tang J, Yan T, Bao Y, Shen C, Yu C, Zhu X, Tian X, Guo F, Liang Q, Liu Q, *et al*: LncRNA GLCC1 promotes colorectal carcinogenesis and glucose metabolism by stabilizing c-Myc. Nat Commun 10: 3499, 2019.
11. Hua Q, Jin M, Mi B, Xu F, Li T, Zhao L, Liu J and Huang G: LINC01123, a c-Myc-activated long non-coding RNA, promotes proliferation and aerobic glycolysis of non-small cell lung cancer through miR-199a-5p/c-Myc axis. J Hematol Oncol 12: 91, 2019.
12. Pan X, Tan J, Tao T, Zhang X, Weng Y, Weng X, Xu J, Li H, Jiang Y, Zhou D and Shen Y: LINC01123 enhances osteosarcoma cell growth by activating the Hedgehog pathway via the miR-516b-5p/Gli1 axis. Cancer Sci 112: 2260-2271, 2021.
13. Zhang M, Han Y, Zheng Y, Zhang Y, Zhao X, Gao Z and Liu X: ZEB1-activated LINC01123 accelerates the malignancy in lung adenocarcinoma through NOTCH signaling pathway. Cell Death Dis 11: 981, 2020.
14. Li JH, Liu S, Zheng LL, Wu J, Sun WJ, Wang ZL, Zhou H, Qu LH and Yang JH: Discovery of protein-lncRNA interactions by integrating large-scale CLIP-Seq and RNA-Seq datasets. Front Bioeng Biotechnol 2: 88, 2015.
15. Wu X, Yan F, Wang L, Sun G, Liu J, Qu M, Wang Y and Li T: MicroRNA: Another pharmacological avenue for colorectal cancer? Front Cell Dev Biol 8: 812, 2020.
16. Huang L, Zhang Y, Li Z, Zhao X, Xi Z, Chen H, Shi H, Xin T, Shen R and Wang T: MiR-4319 suppresses colorectal cancer progression by targeting ABTB1. United European Gastroenterol J 7: 517-528, 2019.
17. Gao J, Li N, Dong Y, Li S, Xu L, Li X, Li Y, Li Z, Ng SS, Sung JJ, *et al*: miR-34a-5p suppresses colorectal cancer metastasis and predicts recurrence in patients with stage II/III colorectal cancer. Oncogene 34: 4142-4152, 2015.
18. Li S, Zhu K, Liu L, Gu J, Niu H and Guo J: lncARSR sponges miR-34a-5p to promote colorectal cancer invasion and metastasis via hexokinase-1-mediated glycolysis. Cancer Sci 111: 3938-3952, 2020.
19. Li Y, Zeng C, Hu J, Pan Y, Shan Y, Liu B and Jia L: Long non-coding RNA-SNHG7 acts as a target of miR-34a to increase GALNT7 level and regulate PI3K/Akt/mTOR pathway in colorectal cancer progression. J Hematol Oncol 11: 89, 2018.
20. Rokavec M, Öner MG, Li H, Jackstadt R, Jiang L, Lodygin D, Kaller M, Horst D, Ziegler PK, Schwitalla S, *et al*: IL-6R/STAT3/miR-34a feedback loop promotes EMT-mediated colorectal cancer invasion and metastasis. J Clin Invest 124: 1853-1867, 2014.
21. Hanahan D and Weinberg RA: Hallmarks of cancer: The next generation. Cell 144: 646-674, 2011.
22. Gatenby RA and Gillies RJ: Why do cancers have high aerobic glycolysis? Nat Rev Cancer 4: 891-899, 2004.

23. Ji S, Zhang B, Liu J, Qin Y, Liang C, Shi S, Jin K, Liang D, Xu W, Xu H, *et al*: ALDOA functions as an oncogene in the highly metastatic pancreatic cancer. Cancer Lett 374: 127-135, 2016.
24. Fu H, Gao H, Qi X, Zhao L, Wu D, Bai Y, Li H, Liu X, Hu J and Shao S: Aldolase A promotes proliferation and G_1/S transition via the EGFR/MAPK pathway in non-small cell lung cancer. Cancer Commun (Lond) 38: 18, 2018.
25. Kukita A, Yoshida MC, Fukushige S, Sakakibara M, Joh K, Mukai T and Hori K: Molecular gene mapping of human aldolase A (ALDOA) gene to chromosome 16. Hum Genet 76: 20-26, 1987.
26. Li H, Zhang X, Jin Z, Yin T, Duan C, Sun J, Xiong R and Li Z: MiR-122 promotes the development of colon cancer by targeting ALDOA in vitro. Technol Cancer Res Treat 18: 1533033819871300, 2019.
27. Dai L, Pan G, Liu X, Huang J, Jiang Z, Zhu X, Gan X, Xu Q and Tan N: High expression of ALDOA and DDX5 are associated with poor prognosis in human colorectal cancer. Cancer Manag Res 10: 1799-1806, 2018.
28. Livak KJ and Schmittgen TD: Analysis of relative gene expression data using real-time quantitative PCR and the 2(-Delta Delta C(T)) method. Methods 25: 402-408, 2001.
29. Tang XJ, Wang W and Hann SS: Interactions among lncRNAs, miRNAs and mRNA in colorectal cancer. Biochimie 163: 58-72, 2019.
30. Heneghan HM, Miller N and Kerin MJ: MiRNAs as biomarkers and therapeutic targets in cancer. Curr Opin Pharmacol 10: 543-550, 2010.
31. Sun DE and Ye SY: Emerging roles of long noncoding RNA regulator of reprogramming in cancer treatment. Cancer Manag Res 12: 6103-6112, 2020.
32. Lin X, Zhuang S, Chen X, Du J, Zhong L, Ding J, Wang L, Yi J, Hu G, Tang G, *et al*: lncRNA ITGB8-AS1 functions as a ceRNA to promote colorectal cancer growth and migration through integrin-mediated focal adhesion signaling. Mol Ther 30: 688-702, 2022.
33. Zhang M, Weng W, Zhang Q, Wu Y, Ni S, Tan C, Xu M, Sun H, Liu C, Wei P and Du X: The lncRNA NEAT1 activates Wnt/β-catenin signaling and promotes colorectal cancer progression via interacting with DDX5. J Hematol Oncol 11: 113, 2018.
34. Qie S and Diehl JA: Cyclin D1, cancer progression, and opportunities in cancer treatment. J Mol Med (Berl) 94: 1313-1326, 2016.
35. Dragutinović VV, Radonjić NV, Petronijević ND, Tatić SB, Dimitrijević IB, Radovanović NS and Krivokapić ZV: Matrix metalloproteinase-2 (MMP-2) and -9 (MMP-9) in preoperative serum as independent prognostic markers in patients with colorectal cancer. Mol Cell Biochem 355: 173-178, 2011.
36. Bao Y, Lu Y, Feng W, Yu H, Guo H, Tao Y, Shi Q, Chen W and Wang X: COUP-TFII promotes epithelial-mesenchymal transition by inhibiting miR-34a expression in colorectal cancer. Int J Oncol 54: 1337-1344, 2019.
37. Lunt SY and Vander Heiden MG: Aerobic glycolysis: Meeting the metabolic requirements of cell proliferation. Annu Rev Cell Dev Biol 27: 441-464, 2011.
38. Tochio T, Tanaka H, Nakata S and Hosoya H: Fructose-1,6-bisphosphate aldolase A is involved in HaCaT cell migration by inducing lamellipodia formation. J Dermatol Sci 58: 123-129, 2010.
39. Kawai K, Uemura M, Munakata K, Takahashi H, Haraguchi N, Nishimura J, Hata T, Matsuda C, Ikenaga M, Murata K, *et al*: Fructose-bisphosphate aldolase A is a key regulator of hypoxic adaptation in colorectal cancer cells and involved in treatment resistance and poor prognosis. Int J Oncol 50: 525-534, 2017.
40. Li X, Zhao S, Fu Y, Zhang P, Zhang Z, Cheng J, Liu L and Jiang H: miR-34a-5p functions as a tumor suppressor in head and neck squamous cell cancer progression by targeting Flotillin-2. Int J Biol Sci 17: 4327-4339, 2021.
41. Yang X, Sun Q, Song Y and Li W: circHUWE1 exerts an oncogenic role in inducing DDP-resistant NSCLC progression depending on the regulation of miR-34a-5p/TNFAIP8. Int J Genomics 2021: 3997045, 2021.

This work is licensed under a Creative Commons Attribution-NonCommercial-NoDerivatives 4.0 International (CC BY-NC-ND 4.0) License.